DALTON
FULL PAPER

1,1′-Bis(2-pyridylthio)ferrocene: a new ligand in gold and silver chemistry

Eva M. Barranco,[a] Olga Crespo,[a] M. Concepción Gimeno,[a] Peter G. Jones,[b] Antonio Laguna *[a] and Cristina Sarroca[a]

[a] *Departamento de Química Inorgánica, Instituto de Ciencia de Materiales de Aragón, Universidad de Zaragoza-CSIC, E-50009 Zaragoza, Spain. E-mail: alaguna@posta.unizar.es*
[b] *Institut für Anorganische und Analytische Chemie der Technischen Universität, Postfach 3329, D-38023 Braunschweig, Germany*

Received 21st March 2001, Accepted 18th June 2001
First published as an Advance Article on the web 10th August 2001

The treatment of $FcLi_2{\cdot}TMDA$ with pyS–Spy (py = 2-pyridyl) leads to the new ferrocene derivative $Fc(Spy)_2$ **1**. The reaction of **1** with gold(I) or gold(III) complexes gives heterometallic complexes of the type $[\{Au(C_6F_5)\}_2\{Fc(Spy)_2\}]$, $[\{Au(PPh_3)\}_2\{Fc(Spy)_2\}](OTf)_2$ or $[\{Au(C_6F_5)_3\}_2\{Fc(Spy)_2\}]$ where the coordination of the gold centres takes place through the nitrogen atoms as evidenced by two crystal structure determinations. Complex **1** also reacts with silver complexes to afford derivatives such as $[Ag(OTf)\{Fc(Spy)_2\}]$, $[Ag(PPh_3)\{Fc(Spy)_2\}]OTf$, $[\{Ag(PPh_3)\}_2\{Fc(Spy)_2\}](OTf)_2$ or $[Ag_2\{Fc(Spy)_2\}_3](OTf)_2$. Substitution of the triflate ligand in $[Ag(OTf)\{Fc(Spy)_2\}]$ by bidentate ligands such as phen or SdppmS gives $[Ag(phen)\{Fc(Spy)_2\}]OTf$ or $[Ag(SdppmS)\{Fc(Spy)_2\}]OTf$. The silver complex $[Ag_2\{Fc(Spy)_2\}_3](OTf)_2$ has also been characterised by X-ray diffraction showing three 1,1′-bis(2-pyridylthio)ferrocene ligands bridging two silver atoms.

Introduction

The chemistry of ferrocene and the design of new compounds containing the ferrocene unit has received much attention, associated with the utility of such products in many fields such as organic synthesis, catalysis and material chemistry.[1–3] Numerous derivatives have been described in which the ferrocene unit is bonded to a fragment containing one or more donor atoms. Studies of these ligands are important because the complexes thus obtained may present interesting redox properties or unusual structures. The study of these compounds, which contain the redox ferrocene unit in close proximity to a second binding site, is of much interest for the development of electronically communicating metal centres and electrochemical sensors.[3–6]

In order to extend the utility of ferrocene as a chelating ligand, we investigated the preparation and reactivity of ferrocenyl thiolate complexes. Several alkyl or arylthioferrocene derivatives have been previously prepared by reaction of 1,1′-dilithioferrocene with the corresponding disulfide[1,7] and some metal complexes of these ligands have been described.[7–10] As far as we are aware no gold or silver derivatives have been reported. As part of our studies of ferrocene derivatives as ligands,[11] we report here on the synthesis of the new ligand 1,1′-bis(2-pyridylthio)ferrocene and some complexation studies with gold and silver. Compared to the disubstituted thioferrocene derivatives, this ligand has the advantage of the presence of the pyridine groups. We have found that the coordination of these metals takes place through the nitrogen atoms, as evidenced by crystal structures. The electrochemical behaviour of the ligand and the complexes has been studied.

Results and discussion

The reaction of ferrocene with LiBu–TMDA followed by addition of dithiodipyrine (pyS–Spy) in a 1 : 2 molar ratio gives the new 1,1′-bis(2-pyridylthio)ferrocene derivative, $Fc(Spy)_2$ **1**, together with two equivalents of LiSpy, that is separated by recyrstallization. Compound **1** is an air- and moisture-stable yellow solid that is non-conducting in acetone solutions. The IR spectrum presents, apart from the typical absorptions of the ferrocene moiety, the bands assigned to ν(C–N) vibrations at 1558 (m) and 1575 (m) cm^{-1}. The ^1H NMR spectrum shows two multiplets, arising from the α and β protons of the substituted cyclopentadienyl groups, and the resonances of the equivalent pyridine protons, which appear as two doublets and two virtual triplets, respectively. In the positive-ion liquid secondary mass spectrum (LSIMS+) the molecular peak appears at $m/z = 404$ (100%) with coincident experimental, calculated and isotopic distributions.

We have studied the reactivity of the new ligand with gold and silver complexes. Thus, treatment of **1** with two equiv. of $[Au(C_6F_5)(tht)]$ (tht = tetrahydrothiophene) affords the neutral complex $[\{Au(C_6F_5)\}_2\{Fc(Spy)_2\}]$ **2** (Scheme 1). We believe that the gold centres are coordinated to the ligand through the nitrogen atoms as found in the crystal structure of complex **3** (see below). This is not surprising if we take into account that thioether derivatives are not such good ligands as other sulfur based ligands. Complex **2** is an air- and moisture-stable yellow solid, non-conducting in acetone solutions. Its IR spectrum shows ν(C–N) vibrations at 1559 (m) and 1599 (m) cm^{-1} and the absorptions due to the pentafluorophenyl group at 1502 (s), 959 (vs) and 807 (s) cm^{-1}. In the ^1H NMR spectrum two multiplets for the α and β protons of the Cp rings and four resonances of the pyridine units are seen. The ^{19}F NMR spectrum shows the typical pattern of a C_6F_5 group with two multiplets for the *ortho* and *meta* fluorine and a triplet for the *para* fluorine. In the positive-ion liquid secondary mass spectrum (LSIMS+) the molecular peak does not appear; the peak arising at the loss of one pentafluorophenyl unit at $m/z = 965$ (10%) and the fragment $[Au(C_6F_5)\{Fc(Spy)_2\}]^+$ at $m/z = 768$ (25%) are observed.

The reaction of **1** with $[Au(OTf)(PPh_3)]$ in molar ratio 2 : 1 gives the cationic complex $[\{Au(PPh_3)\}_2\{Fc(Spy)_2\}](OTf)_2$ **3** (Scheme 1). Compound **3** is an air- and moisture-stable orange solid that behaves as a 2 : 1 electrolyte in acetone solutions. Its IR spectrum shows ν(C–N) vibrations at 1518 (m) and 1598 (m)

DOI: 10.1039/b102636b

cm^{-1}; the bands for the trifluoromethanesulfonate (triflate) anion appear at 1264 (vs), 1224 (s) and 1155 (s) cm^{-1}. The ^{1}H NMR spectrum presents a similar pattern to the compounds mentioned above but with different chemical shifts; the ^{31}P{^{1}H} NMR spectrum shows one singlet for the two equivalent phosphorus atoms. In the LSIMS+ the fragment [Au(PPh$_3$)-{Fc(Spy)$_2$}]$^+$ at *m*/*z* = 863 (40%), arising by the loss of the triflate anions and one Au(PPh$_3$)$^+$ group, is observed, but the molecular peak is not.

The structure of complex **3** has been confirmed by an X-ray diffraction study, and the cation is shown in Fig. 1. A selection of bond lengths and angles is collected in Table 1. The iron atom lies on a symmetry centre and thus only half of the molecule corresponds to the asymmetric unit. The coordination of the gold centres to the ligand takes place through the nitrogen atoms with an angle N–Au–P of 178.0(2)° very close to the ideal value. The Au–S1 distance is 3.154 Å and is too long to be considered as any significant bonding interaction, as evidenced by the linearity at the gold atom. The Au–N distance is 2.083(6) Å and is of the same order as those found in other gold(I) complexes containing nitrogen ligands, such as [Au(PPh$_3$)-(dmpy)]ClO$_4$ (dmpy = 2,6-dimethylpyridine) (2.091(13) Å),[12] [Au(Fcpy)(PPh$_3$)]OTf (Fcpy = 3-ferrocenylpyridine) (2.065(10) and 2.070(9) Å, two independent molecules)[13] or [FcCHN-(AuPPh$_3$)(CH$_2$)$_2$S(AuPPh$_3$)$_2$](OTf)$_2$ (2.100(12) Å).[14] The Au–P distance, 2.242(2) Å, is also similar to that found in the latter compounds for the N–Au–P moiety.

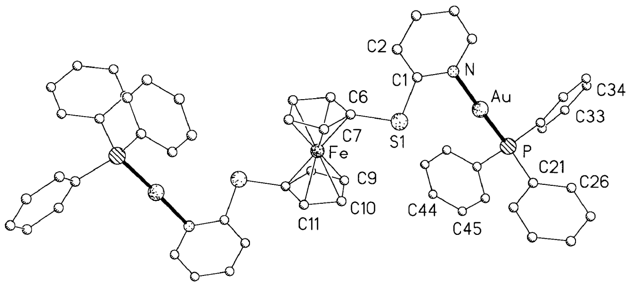

Fig. 1 The structure of the cation of complex **3** in the crystal, showing the atom numbering scheme of the asymmetric unit; H atoms are omitted for clarity.

Table 1 Selected bond lengths (Å) and angles (°) for complex **3**

Au–N	2.083(6)	N–C(1)	1.357(9)
Au–P	2.2420(17)	S(1)–C(6)	1.762(8)
N–C(5)	1.356(9)	S(1)–C(1)	1.770(7)
N–Au–P	178.01(17)	C(6)–S(1)–C(1)	102.2(3)
C(21)–P–Au	112.2(2)	N–C(1)–C(2)	120.7(6)
C(31)–P–Au	111.9(2)	N–C(1)–S(1)	113.5(5)
C(41)–P–Au	111.5(2)	C(2)–C(1)–S(1)	125.8(6)
C(5)–N–C(1)	120.1(6)	N–C(5)–C(4)	120.3(7)
C(5)–N–Au	118.5(5)	C(10)–C(6)–S(1)	126.6(6)
C(1)–N–Au	121.3(4)	C(7)–C(6)–S(1)	125.0(6)

Because of imposed symmetry the cyclopentadienyl rings are planar and they adopt an ideal antiperiplanar disposition; the gold atoms are located in opposite directions and no gold–gold interactions are possible. The sulfur atoms lie 0.14 Å out of the planes formed by the cyclopentadienyl groups, pointed towards the iron atom.

We have also synthesized the gold(III) derivative [{Au-(C$_6$F$_5$)$_3$}$_2${Fc(Spy)$_2$}] **4** by reaction of Fc(Spy)$_2$ with two equiv. of [Au(C$_6$F$_5$)$_3$OEt$_2$] (Scheme 1). Complex **4** is an air- and moisture-stable orange solid that is non-conducting in acetone solutions. Its IR spectrum shows the *ν*(C–N) bands of the ferrocene ligand at 1558 (m) and 1576 (m) cm^{-1}; those arising at the pentafluorophenyl groups bonded to a gold(III) centre appear at 1510 (s), 970 (s), 816 (m) and 796 (m) cm^{-1}.

The ^{1}H NMR spectrum shows two multiplets for the α and β protons of the Cp rings and the resonances of the pyridine protons. The ^{19}F NMR spectrum presents the typical pattern for equivalent "Au(C$_6$F$_5$)$_3$" groups, which consists of six signals in a 2 : 1 ratio for the mutually *trans* and *cis* pentafluorophenyl groups, respectively. In the LSIMS+ the molecular peak does not appear, but the peak arising at the loss of one Au(C$_6$F$_5$)$_3$ group at *m*/*z* = 1103 (15%) is observed.

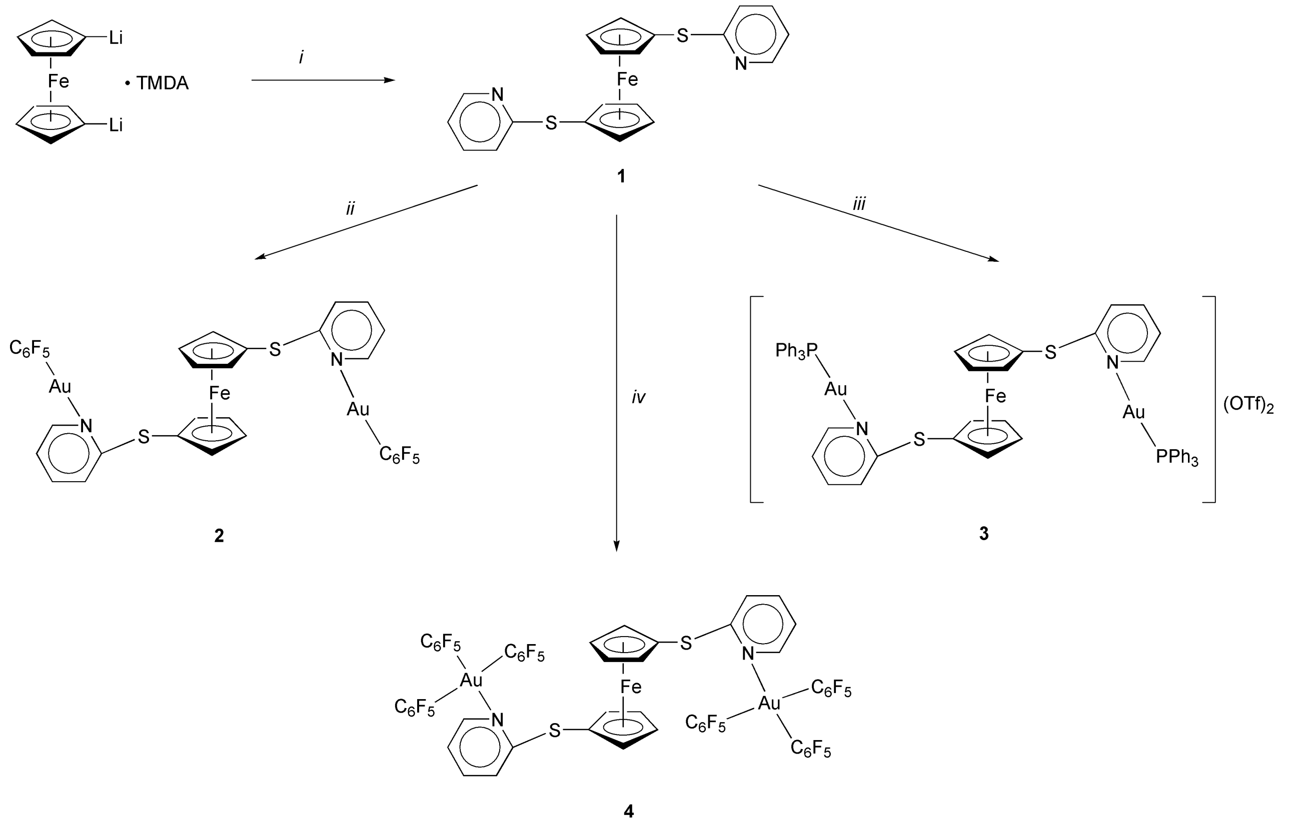

Scheme 1 Reagents and conditions: *i*, 2 pySSpy; *ii*, 2 [Au(C$_6$F$_5$)(tht)]; *iii*, 2 [Au(OTf)(PPh$_3$)]; *iv*, 2 [Au(C$_6$F$_5$)$_3$(OEt$_2$)].

Table 2 Selected bond lengths (Å) and angles (°) for complex **4**

Au–C(21)	2.005(5)	S–C(51)	1.742(6)
Au–C(11)	2.058(6)	S–C(42)	1.755(5)
Au–C(31)	2.077(6)	N(41)–C(42)	1.346(7)
Au–N(41)	2.105(4)	N(41)–C(46)	1.355(6)
C(21)–Au–C(11)	88.2(2)	C(12)–C(11)–Au	123.9(4)
C(21)–Au–C(31)	88.4(2)	C(16)–C(11)–Au	120.7(4)
C(11)–Au–C(31)	176.0(2)	C(36)–C(31)–Au	119.6(5)
C(21)–Au–N(41)	177.8(2)	C(32)–C(31)–Au	123.9(5)
C(11)–Au–N(41)	92.1(2)	C(42)–N(41)–Au	121.7(3)
C(31)–Au–N(41)	91.3(2)	C(46)–N(41)–Au	119.3(4)

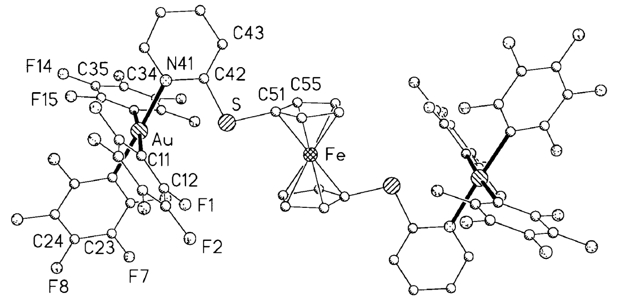

Fig. 2 Perspective view of complex **4**, with the atom labeling scheme; H atoms are omitted for clarity.

The structure of complex **4** has been confirmed by an X-ray diffraction study and the molecule is shown in Fig. 2. Selected bond lengths and angles are collected in Table 2. The molecule displays crystallographic inversion symmetry. The gold atom has the expected square planar geometry; the mean deviation of the plane formed by the four donor atoms is 0.04 Å. The angles around the gold atom are also very regular and close to the ideal values, mean deviation 2.1°. The sulfur atom is 3.124 Å away from the gold(III) centre but the position should be attributed more to the rigidity of the ligand than to any significant bonding interaction. The Au–C distances to mutually *trans* pentafluorophenyl groups are 2.058(6) and 2.077(6) Å and are very similar to those observed in the complex $[Au(C_6F_5)_3(FcPy)]$[13] which has a similar skeleton. The shortest Au–C distance of 2.005(5) Å reflects the higher *trans* influence of the pentafluorophenyl ligand compared to the nitrogen ligands. The Au–N bond length is also comparable to that in the compound $[Au(C_6F_5)_3(FcPy)]$ (2.103(3) Å).[13] Again because of imposed symmetry the cyclopentadienyl rings are planar and they adopt an ideal antiperiplanar disposition. The sulfur atoms lie 0.29 Å out of the planes formed by the cyclopentadienyl groups, pointed towards the iron atom.

We have also carried out reactions of **1** with silver complexes such as $[Ag(OTf)(PPh_3)]$ in 1 : 1 and 1 : 2 molar ratio to give the complexes $[Ag(PPh_3)\{Fc(Spy)_2\}]OTf$ **5** or $[\{Ag(PPh_3)\}_2\{Fc(Spy)_2\}](OTf)_2$ **6** (Scheme 2). Complexes **5** and **6** are air- and moisture-stable yellow solids that behave as 1 : 1 or 1 : 2 electrolytes, respectively. Their IR spectra show the *ν*(C–N) bands at 1562 (m) and 1585 (m) for **5** and 1562 (m) and 1588 (m) cm^{-1} for **6**; in both the bands arising at the ionic trifluoromethanesulfonate appear at around 1264 (vs, br), 1224 (s) and 1155 (s) cm^{-1}.

The ^1H NMR spectra present the resonances for the cyclopentadienyl, phenylic and pyridine protons in the appropriate ratio for one or two $AgPPh_3$ units. The $^{31}P\{^1H\}$ NMR spectra at room temperature consist of a broad multiplet that splits at −55 °C into two doublets as a consequence of the coupling of phosphorus atoms with both silver nuclei, ^{107}Ag and ^{109}Ag.

In the positive-ion mass spectra the cation molecular peaks arising by the loss of one triflate anion appear for complex **5** at *m*/*z* = 773 (45 %) and for complex **6** at *m*/*z* = 1293 (2%). In both cases the most intense peak corresponds to the fragment $[Ag\{Fc(Spy)_2\}]^+$ at *m*/*z* = 511.

Table 3 Selected bond lengths (Å) and angles (°) for complex **8**[a]

Ag–N(1)	2.292(7)	S(3)–C(21)	1.750(8)
Ag–N(2)	2.311(6)	S(3)–C(41)	1.786(10)
Ag–N(3)	2.321(8)	N(1)–C(15)	1.350(10)
S(1)–C(1)	1.758(9)	N(2)–C(31)	1.322(11)
S(1)–C(11)	1.787(8)	N(2)–C(35)	1.345(10)
S(2)–C(31)	1.794(10)	N(3)–C(45)	1.345(11)
S(2)–C(6)#1	1.822(9)	N(3)–C(41)	1.349(11)
N(1)–Ag–N(2)	120.1(2)	C(31)–N(2)–Ag	116.6(5)
N(1)–Ag–N(3)	113.9(3)	C(35)–N(2)–Ag	124.5(6)
N(2)–Ag–N(3)	124.7(3)	C(45)–N(3)–Ag	118.2(6)
C(11)–N(1)–Ag	120.6(5)	C(41)–N(3)–Ag	123.5(6)
C(15)–N(1)–Ag	120.3(6)		

[a] Symmetry transformations used to generate equivalent atoms: #1 $-x + 1, y, -z + 1/2$.

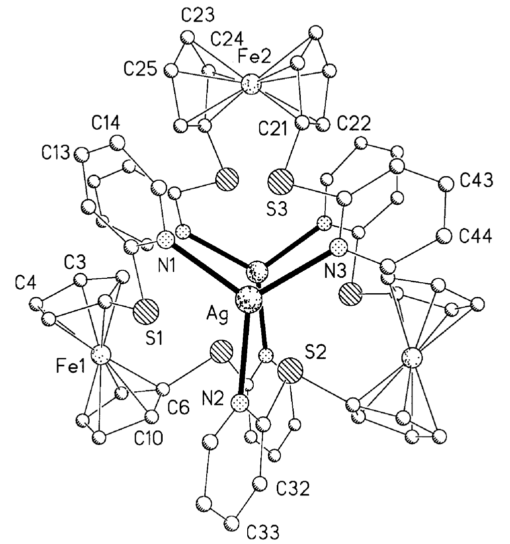

Fig. 3 Structure of the cation of complex **8** in the crystal, showing the atom numbering scheme; H atoms are omitted for clarity.

The reaction of **1** with AgOTf has been carried out in a 1 : 1 and 3 : 2 molar ratio and gives the compounds $[Ag(OTf)\{Fc(Spy)_2\}]$ **7** or $[Ag_2\{Fc(Spy)_2\}_3](OTf)_2$ **8**, respectively (Scheme 2). In complex **7** we propose that the silver atom is bonded to both nitrogen atoms of the ligand, acting as a chelate, and to the oxygen atom of the trifluoromethanesulfonate anion. In compound **8** both silver centres are three-coordinated and bonded to one nitrogen atom of the three different ligands (see X-ray discussion below).

The IR spectra of **7** and **8** show the absorptions of the triflate anion bonded to silver at 1223 (vs, br), 1199 (s) and 1151 (s) cm^{-1} for **7**, which are characteristic of coordinated triflate, or for compound **8** the typical values for a counteranion. The ν(C–N) vibration appears at 1562 (s) and 1576 (s) cm^{-1} for **7** and **8**, respectively.

The structure of compound **8** has been established by an X-ray diffraction study. Suitable crystals were obtained from chloroform–hexane. The cation is shown in Fig. 3; it displays twofold symmetry, with the atom Fe2 lying on the special position 0.5, *y*, 0.25. A selection of bond lengths and angles is collected in Table 3. The two silver atoms have a trigonal planar geometry, bonded to three nitrogen atoms with the 1,1′-bis(2-pyridylthio)ferrocene derivatives acting as bridging ligands. The Ag–N distances are 2.292(7), 2.311(6) and 2.321(8) Å and these are similar to those found in other three-coordinated silver derivatives such as $[Ag_2(pyz)_3](BF_4)_2$ (pyz = pyrazine) (2.280(2), 2.245(2) and 2.419(3) Å).[15] The N–Ag–N angles are 120.1(2), 113.9(3) and 124.7(3) ° which are very close to the ideal values. The Ag–S distances are too long to consider any

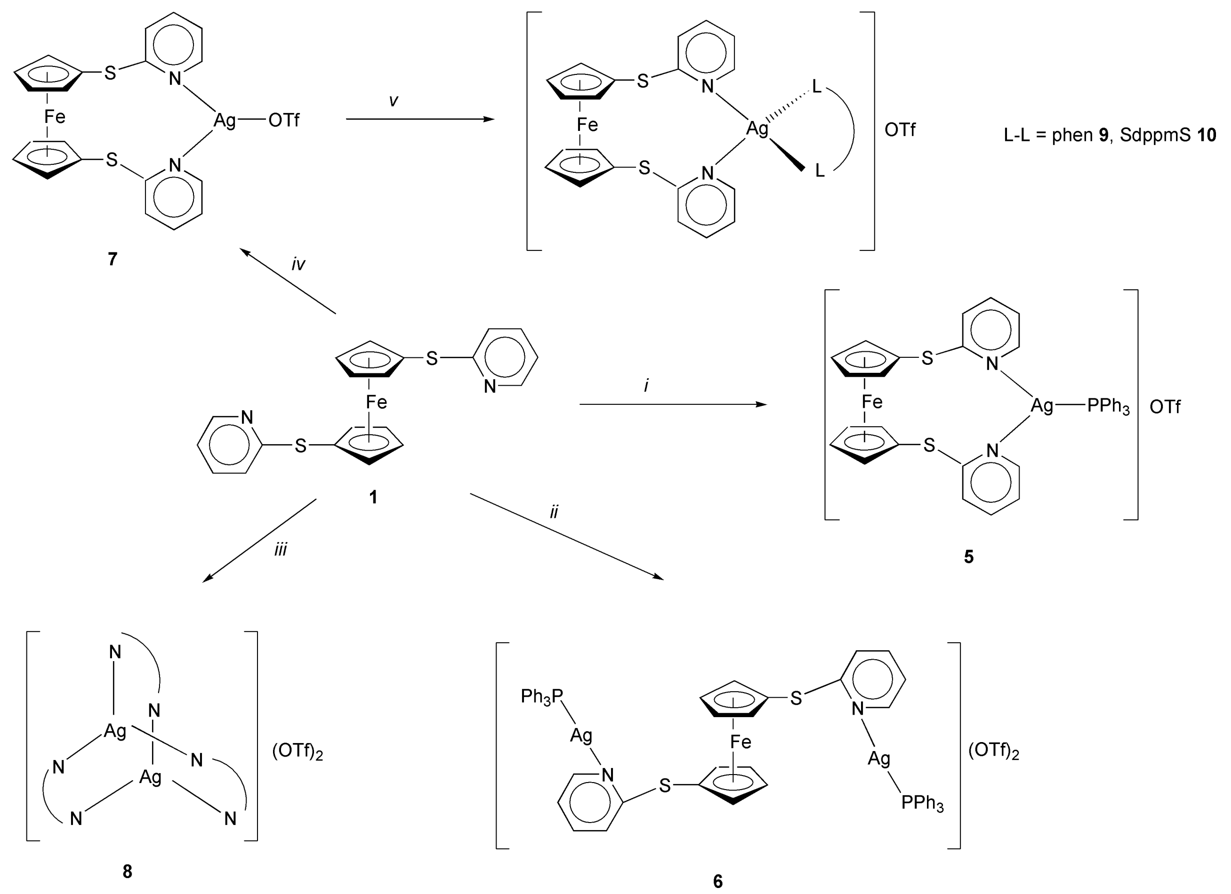

Scheme 2 Reagents and conditions; *i*, [Ag(OTf)(PPh$_3$)]; *ii*, 2 [Ag(OTf)(PPh$_3$)]; *iii*, 2/3 AgOTf; *iv*, AgOTf; *v*, phen or SdppmS.

bonding interaction. The cyclopentadienyl rings adopt an almost eclipsed geometry with the interplanar angles for the ferrocenes of 3.4° for Fe1 and 3.1° for Fe2.

Complex **7** possesses a weakly coordinating ligand in trifluoromethanesulfonate and thus can further react with other ligands such as 1,10-phenanthroline (phen) or bis(diphenylphosphino)methane disulfide (SdppmS) affording the complexes [Ag(phen){Fc(Spy)$_2$}]OTf **9** or [Ag(SdppmS){Fc(Spy)$_2$}]OTf **10**. Complexes **9** and **10** are yellow air- and moisture-stable solids that behave as 1 : 1 electrolytes in acetone solutions.

The ^{1}H NMR spectra of **9** and **10** present only one multiplet for the cyclopentadienyl ligands and the characteristic resonances of the thiopyridine groups. The spectrum of complex **9** also shows four signals for the phenanthroline protons and compound **10** a triplet for the methylene protons because of the coupling with the phosphorus atoms. The ^{31}P(^{1}H) NMR spectrum of **10** presents a singlet for the equivalent phosphorus atoms. In the mass spectra (LSIMS+) the cation molecular peaks appear at $m/z = 692$ (21%) and 960 (2%) for **9** and **10**, respectively.

Electrochemistry

The electrochemical behaviour of the ligand and the gold and silver derivatives has been studied by cyclic voltammetry at a platinum electrode in CH$_2$Cl$_2$. The free ligand undergoes a quasi-reversible one-electron oxidation process, based on the ferrocene unit, at a potential slightly higher than the free ferrocene unit. It also shows one further anodic irreversible wave that could be due to a chemical reaction probably involving the thiopyridine substituents. (see Fig. 4). This behaviour has been observed for ferrocenylphosphine derivatives such as 1,1′-bis(diphenylphosphino)ferrocene.[16] The coordination of gold and silver to the new ligand makes the redox properties of the complexes markedly different because the ferrocene redox couple is shifted to higher potentials. The reason for this difference in the electrochemical behaviour is the presence of conjugated π-electron systems between the two metals which allows communication.[3,17,18] The electron-withdrawing nature of the coordinated metal centres makes the ferrocene unit harder to oxidize. The gold(I) complexes show a similar pattern to that of the ligand, although now the ferrocenium–ferrocene couple is shifted to a more anodic potential, and also the oxidation peak that now is on the limit of solvent breakdown. The gold(III) derivative presents only one reversible wave for the ferrocene unit not followed by any chemical reaction, this is probably due to the higher stability of the gold(III) derivative, because the Au(III)–N bond is stronger than the corresponding Au(I)–N. The silver complexes present a more complicated pattern because of the presence of one or two silver(I) atoms that can be oxidized to Ag^{2+}, although only one large wave appears for each compound. Table 4 collects the electrochemical data for these compounds.

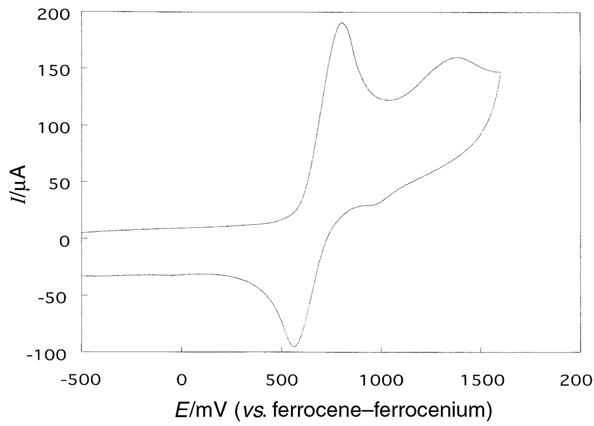

Fig. 4 Cyclic voltammogram of ligand **1** *vs.* ferrocene–ferrocenium.

Table 4 Electrochemical data for compounds **1**–**8**

Compound	E_1/V	E_{ox}/V
1 Fc(Spy)$_2$	0.65	1.16
2 [{Au(C$_6$F$_5$)}$_2${Fc(Spy)$_2$}]	0.93	1.35
3 [{Au(PPh$_3$)}$_2${Fc(Spy)$_2$}](OTf)$_2$	0.89	1.4
4 [{Au(C$_6$F$_5$)$_3$}$_2${Fc(Spy)$_2$}]	1.06	—
6 [{Ag(PPh$_3$)}$_2${Fc(Spy)$_2$}](OTf)$_2$	0.79	1.18
7 [Ag(OTf){Fc(Spy)$_2$}]	0.74	1.18
8 [Ag$_2${Fc(Spy)$_2$}$_3$](OTf)$_2$	0.83	1.17

Experimental

Instrumentation

Infrared spectra were recorded in the range 4000–200 cm^{-1} on a Perkin-Elmer 883 spectrophotometer using Nujol mulls between polyethylene sheets. Conductivities were measured in *ca.* 5×10^{-4} mol dm^{-3} solutions with a Philips 9509 conductimeter. C, H and S analyses were carried out with a Perkin-Elmer 2400 microanalyzer. Mass spectra were recorded on a VG Autospec, with the LSIMS technique, using nitrobenzyl alcohol as matrix. NMR spectra were recorded on a Varian Unity 300 spectrometer and a Bruker ARX 300 spectrometer in CDCl$_3$. Chemical shifts are cited relative to SiMe$_4$ (^{1}H, external), CFCl$_3$ (19F, external), and 85% H$_3$PO$_4$ (^{31}P, external). Cyclic voltammetric experiments were performed by employing an EG&G PARC model 273 potentiostat. A three-electrode system was used, which consists of a platinum disk working electrode. The measurements were carried out in CH$_2$Cl$_2$ solutions with 0.1 mol dm^{-3} Bu$_4$NPF$_6$ as a supporting electrolyte. Under the present experimental conditions, the ferrocenium–ferrocene couple was located at 0.47 V *vs.* SCE.

Materials

The starting materials [Au(C$_6$F$_5$)(tht)][19] and [Au(C$_6$F$_5$)$_3$(OEt$_2$)][20] were prepared by published procedures. [Au(OTf)(PPh$_3$)] was prepared from [AuCl(PPh$_3$)][21] and AgOTf in dichloromethane and [Ag(OTf)PPh$_3$] was obtained from AgOTf and PPh$_3$ in dichloromethane. All other reagents were commercially available.

Syntheses

Fc(Spy)$_2$ 1. Ferrocene (1.30 g, 7 mmol) was added to a solution of *N*,*N*,*N′*,*N′*-tetramethylethylenediamine (TMDA) (4 cm^3, 20 mmol) and 1.44 mol dm^{-3} *n*-butyllithium in hexane (14 cm^3, 20 mmol) in oxygen-free hexane (50 cm^3) in a 250 cm^3 round-bottom flask equipped with a side arm and serum cap, under nitrogen. The solution was stirred overnight. The hexane was removed *via* syringe and the solid was washed twice with hexane (2×20 cm^3) in order to remove unreacted ferrocene. Then 60 cm^3 of hexane were added, the mixture cooled to 0 °C and a solution of 2,2′-dithiodipyridine (3.08 g, 14 mmol) in toluene added *via* dropping funnel. The mixture containing Fc(Spy)$_2$ was stirred for 8 h and then the solid was filtered off and recrystallised from dichloromethane–hexane to give compound **1** as a brown-orange solid. Yield 53%. Λ_M 0.64 Ω^{-1} cm^2 mol^{-1} (Found: C, 58.98; H, 3.75; N, 6.96; S, 15.65. Calc. for C$_{20}$H$_{16}$FeN$_2$S$_2$: C, 59.40; H, 3.98; N, 6.92; S, 15.85%). ^{1}H NMR, δ 4.48 (m, 4H, C$_5$H$_4$), 4.52 (m, 4H, C$_5$H$_4$), 6.79 (d, 2H, py, *J*(HH) 8.06 Hz), 6.90 (dd, 2H, py, *J*(HH) 8.06, 4.88 Hz), 7.38 (virtual t, 2H, py, *J*(HH) 4.5 Hz), 8.33 (d, 2H, py, 3.2 Hz).

[{Au(C$_6$F$_5$)}$_2${Fc(Spy)$_2$}] 2. To a solution of Fc(Spy)$_2$ (0.040 g, 0.1 mmol) in dichloromethane (20 cm^3) was added [Au(C$_6$F$_5$)(tht)] (0.090 g, 0.2 mmol) and the mixture was stirred for 30 min. Evaporation of the solvent to *ca.* 5 cm^3 and addition of hexane afforded complex **2** as an orange solid. Yield 64%. Λ_M 8 Ω^{-1} cm^2 mol^{-1} (Found: C, 33.61; H, 1.11; N, 2.54; S, 5.92. Calc. for C$_{32}$H$_{16}$Au$_2$F$_{10}$FeN$_2$S$_2$: C, 33.94; H, 1.14; N, 2.47; S, 5.66%). ^{1}H NMR, δ 4.61 (m, 4H, C$_5$H$_4$), 4.64 (m, 4H, C$_5$H$_4$), 6.98 (d, 2H, py, *J*(HH) 8.39 Hz), 7.17 (virtual t, 2H, py, *J*(HH) ≈ 7.5 Hz), 7.63 (virtual t, 2H, py, *J*(HH) 8.02 Hz), 8.39 (d, 2H, py, *J*(HH) 5.53 Hz). ^{19}F NMR, δ −116.6 (m, 4F, *o*-F), −163.4 (m, 4F, *m*-F), −159.8 [t, 2F, *p*-F, ^{3}*J*(FF) 18.9 Hz].

[{Au(PPh$_3$)}$_2${Fc(Spy)$_2$}](OTf)$_2$ 3. To a solution of Fc(Spy)$_2$ (0.040 g, 0.1 mmol) in dichloromethane (20 cm^3) was added [Au(OTf)PPh$_3$] (0.122 g, 0.2 mmol) and the mixture was stirred for 30 min. Evaporation of the solvent to *ca.* 5 cm^3 and addition of diethyl ether afforded complex **3** as a yellow solid. Yield 67%. Λ_M 204.2 Ω^{-1} cm^2 mol^{-1} (Found: C, 43.03; H, 2.53; N, 1.54; S, 7.87. Calc. for C$_{58}$H$_{46}$Au$_2$F$_6$FeN$_2$O$_6$P$_2$S$_4$: C, 42.97; H, 2.86; N, 1.65; S, 7.91%). ^{1}H NMR, δ 4.53 (m, 8H, C$_5$H$_4$), 7.03 (d, 2H, py, *J*(HH) 8.17 Hz), 7.4–7.6 (m, 30 + 2H, py + Ph), 7.86 (virtual t, 2H, py, *J*(HH) 6.84 Hz), 8.66 (d, 2H, py, 5.38 Hz). ^{31}P{^{1}H} NMR, δ 29.5 (s, 2P, PPh$_3$).

[{Au(C$_6$F$_5$)$_3$}$_2${Fc(Spy)$_2$}] 4. To a solution of Fc(Spy)$_2$ (0.040 g, 0.1 mmol) in dichloromethane (20 cm^3) was added [Au(C$_6$F$_5$)$_3$-(OEt$_2$)] (0.154 g, 0.2 mmol) and the mixture was stirred for 30 min. Evaporation of the solvent to *ca.* 5 cm^3 and addition of hexane afforded complex **4** as a yellow solid. Yield 84%. Λ_M 15 Ω^{-1} cm^2 mol^{-1} (Found: C, 37.61; H, 1.01; N, 1.54; S, 3.92. Calc. for C$_{56}$H$_{16}$Au$_2$F$_{30}$FeN$_2$S$_2$: C, 37.35; H, 0.89; N, 1.55; S, 3.56%). ^{1}H NMR, δ 4.48 (m, 4H, C$_5$H$_4$), 4.52 (m, 4H, C$_5$H$_4$), 6.80 (d, 2H, py, *J*(HH) 8.06 Hz), 6.91 (virtual t, 2H, py, *J*(HH) 7.21 Hz), 7.36 (virtual t, 2H, py, *J*(HH) 7.57 Hz), 8.33 (d, 2H, py, *J*(HH) 4.52 Hz). ^{19}F NMR, δ −120.0 (m, 4F, *o*-F), −122.1 (m, 2F, *o*-F), −161.1 (m, 4F, *m*-F), −161.2 (m, 2F, *m*-F), −156.3 [t, 2F, *p*-F, ^{3}*J*(FF) 19.3 Hz], −157.1 [t, 1F, *p*-F, ^{3}*J*(FF) 19.3 Hz].

[Ag(PPh$_3$){Fc(Spy)$_2$}]OTf 5. To a solution of Fc(Spy)$_2$ (0.040 g, 0.1 mmol) in dichloromethane (20 cm^3) was added [Ag(OTf)PPh$_3$] (0.052 g, 0.1 mmol) and the mixture stirred for 30 min. Evaporation of the solvent to *ca.* 5 cm^3 and addition of diethyl ether afforded a yellow solid of complex **5**. Yield 66%. Λ_M 108 Ω^{-1} cm^2 mol^{-1} (Found: C, 50.23; H, 2.90; N, 2.97; S, 10.47. Calc. for C$_{39}$H$_{31}$AgF$_3$FeN$_2$O$_3$PS$_3$: C, 50.71; H, 3.38; N, 3.03; S, 10.41%). ^{1}H NMR, δ 4.34 (m, 8H, C$_5$H$_4$), 6.79 (d, 2H, py, *J*(HH) 8.02 Hz), 7.06 (virtual t, 2H, py, *J*(HH) 5.68 Hz), 7.4–7.8 (m, 30 + 2H, py + Ph), 8.66 (d, 2H, py, *J*(HH) 4.54 Hz). ^{31}P{^{1}H} NMR (−55 °C), δ 13.6 (2d, 1P, PPh$_3$, *J*(^{109}AgP) 759.8, *J*(^{107}AgP) 657.9 Hz).

[{Ag(PPh$_3$)}$_2${Fc(Spy)$_2$}](OTf)$_2$ 6. To a solution of Fc(Spy)$_2$ (0.040 g, 0.1 mmol) in dichloromethane (20 cm^3) was added [Ag(OTf)(PPh$_3$)] (0.104 g, 0.2 mmol) and the mixture was stirred for 30 min. Evaporation of the solvent to *ca.* 5 cm^3 and addition of diethyl ether afforded complex **6** as a yellow solid. Yield 95%. Λ_M 165 Ω^{-1} cm^2 mol^{-1} (Found: C, 48.14; H, 3.09; N, 2.17; S, 9.25. Calc. for C$_{58}$H$_{46}$Ag$_2$F$_6$FeN$_2$O$_6$P$_2$S$_4$: C, 48.28; H, 3.21; N, 1.94; S, 8.88%). ^{1}H NMR, δ 4.31 (m, 8H, C$_5$H$_4$), 6.79 (d, 2H, py, *J*(HH) 8.01 Hz), 7.08 (virtual t, 2H, py, *J*(HH) 6.25 Hz), 7.4–7.6 (m, 30 + 2H, py + Ph), 8.57 (d, 2H, py, *J*(HH) 4.47 Hz). ^{31}P{^{1}H} NMR (−55 °C), δ 18.2 (2d, 2P, PPh$_3$, *J*(^{109}AgP) 735.1, *J*(^{107}AgP) 639.9 Hz).

[Ag(OTf){Fc(Spy)$_2$}] 7. To a solution of Fc(Spy)$_2$ (0.040 g, 0.1 mmol) in diethyl ether (20 cm^3) was added AgOTf (0.025 g, 0.1 mmol) and the mixture was stirred for 1 h, during which time a yellow precipitate appeared. The solid, complex **7**, was filtered off. Yield 90%. Λ_M 10.6 Ω^{-1} cm^2 mol^{-1} (Found: C, 38.34; H, 2.15; N, 4.41; S, 14.38. Calc. for C$_{21}$H$_{16}$AgF$_3$FeN$_2$O$_3$S$_3$: C, 38.14; H, 2.43; N, 4.23; S, 14.54%). ^{1}H NMR, δ 4.36 (m, 4H, C$_5$H$_4$), 4.44 (m, 4H, C$_5$H$_4$), 6.84 (d, 2H, py, *J*(HH) 8.06 Hz), 7.10 (virtual t, 2H, py, *J*(HH) 6.71 Hz), 7.51 (virtual t, 2H, py, *J*(HH) 7.93 Hz), 8.61 (d, 2H, py, 4.52 Hz).

Table 5 Details of data collection and structure refinement for complexes **3**, **4** and **8**

Compound	**3**	**4**	**8**·5CHCl$_3$
Chemical formula	$C_{58}H_{46}Au_2F_6FeN_2O_6P_2S_4$	$C_{62}H_{30}Au_2F_{30}FeN_2S_2$	$C_{67}H_{53}Ag_2Cl_{15}F_6Fe_3N_6O_6S_8$
M	1620.93	1886.78	2325.69
Crystal habit	Orange plate	Orange prism	Yellow prism
Crystal size/mm	0.75 × 0.20 × 0.05	0.60 × 0.30 × 0.25	0.40 × 0.30 × 0.20
λ/Å	0.71073	0.71073	0.71073
Crystal system	Triclinic	Triclinic	Monoclinic
Space group	$P\bar{1}$	$P\bar{1}$	$C2/c$
a/Å	8.954(1)	9.245(2)	28.074(9)
b/Å	9.981(1)	12.787(2)	13.025(4)
c/Å	17.050(2)	13.500(2)	26.836(9)
α/°	90.01(1)	82.283(10)	90
β/°	98.83(1)	78.168(12)	113.83(2)
γ/°	103.09(1)	74.357(10)	90
U/Å^3	1465.6(3)	1498.9(4)	8976(5)
Z	1	1	4
D_c/g cm^{-3}	1.837	2.090	1.721
F(000)	788	902	4624
T/°C	−100	−100	−100
$2\theta_{max}$/°	50	50	45
μ(Mo-Kα)/cm^{-1}	55.05	53.29	15.97
Transmission	0.667–0.104	0.854–1.000	0.567–0.740
No. of reflections measured	6966	5620	7359
No. of unique reflections	5120	5261	5855
R_{int}	0.0358	0.0178	0.093
$R^a(F > 4\sigma(F))$	0.043	0.0323	0.061
$wR^b(F^2$, all refl.)	0.112	0.0763	0.161
No. of reflections used	5116	5261	5855
No. of parameters	367	433	528
No. of restraints	0	392	309
S^c	1.023	0.956	0.905
Max. $\Delta\rho/e\ \AA^{-3}$	2.624	1.048	1.484

[a] $R(F) = \Sigma \| F_o| - |F_c\| / \Sigma |F_o|$. [b] $wR(F^2) = [\Sigma\{w(F_o^2 - F_c^2)^2\}/\Sigma\{w(F_o^2)^2\}]^{0.5}$; $w^{-1} = \sigma^2(F_o^2) + (aP)^2 + bP$, where $P = [F_o^2 + 2F_c^2]/3$ and a and b are constants adjusted by the program. [c] $S = [\Sigma\{w(F_o^2 - F_c^2)^2\}/(n - p)]^{0.5}$, where n is the number of data and p the number of parameters.

[Ag$_2${Fc(Spy)$_2$}$_3$](OTf)$_2$ 8. To a solution of Fc(Spy)$_2$ (0.121 g, 0.3 mmol) in diethyl ether (20 cm^3) was added Ag(OTf) (0.051 g, 0.2 mmol) and the mixture stirred for 1 h, during which time a yellow precipitate appeared. The solid, complex **8**, was filtered off. Yield 91%. Λ_M 156.4 Ω^{-1} cm^2 mol^{-1} (Found: C, 42.67; H, 2.13; N, 5.05; S, 14.23. Calc. for $C_{62}H_{48}Ag_2F_6Fe_3N_6O_6S_8$: C, 43.12; H, 2.80; N, 4.86; S, 14.86%). ^{1}H NMR, δ 4.37 (m, 4H, C_5H_4), 4.44 (m, 4H, C_5H_4), 6.85 (d, 2H, py), 7.10 (virtual t, 2H, py), 7.51 (virtual t, 2H, py), 8.61 (d, 2H, py).

[Ag(L–L){Fc(Spy)$_2$}]OTf (L–L = phen 9, SdppmS 10). To a solution of complex **7** (0.066 g, 0.1 mmol) in dichloromethane (20 cm^3) was added the bidentate ligand, phen (0.018 g, 0.1 mmol) or SdppmS (0.049 g, 0.1 mmol) and the mixture was stirred for 2 h. Evaporation of the solvent to *ca.* 5 cm^3 and addition of diethyl ether gave complexes **9** or **10** as yellow solids. Complex **9**: yield 64%. Λ_M 109.2 Ω^{-1} cm^2 mol^{-1} (Found: C, 47.32; H, 3.01; N, 6.45; S, 10.93. Calc. for $C_{33}H_{24}AgF_3FeN_4O_3S_3$: C, 47.07; H, 3.11; N, 6.65; S, 11.42%). ^{1}H NMR, δ 4.54 (m, 8H, C_5H_4), 6.89 (d, 2H, py, J(HH) 8.2 Hz), 7.04 (virtual t, 2H, py, J(HH) 6.67 Hz), 7.52 (virtual t, 2H, py, J(HH) 7.02 Hz), 8.41 (d, 2H, py, J(HH) 4.53 Hz), 7.90 (m, 2H, phen), 7.98 (s, 2H, phen), 8.10 (s, 2H, phen), 9.17 (br, 2H, phen). Complex **10**: yield 56%. Λ_M 133 Ω^{-1} cm^2 mol^{-1} (Found: C, 49.26; H, 3.22; N, 2.17; S, 14.31. Calc. for $C_{46}H_{38}AgF_3FeN_2O_3P_2S_5$: C, 49.78; H, 3.45; N, 2.52; S, 14.44%). ^{1}H NMR, δ 4.41 (t, 2H, CH_2), 4.52 (m, 8H, C_5H_4), 6.79 (d, 2H, py, J(HH) 8.02 Hz), 6.93 (virtual t, 2H, py, J(HH) 7.52 Hz), 7.2–7.7 (m, 2 + 20H, py, Ph), 8.10 (d, 2H, py, J(HH) 5.02 Hz). ^{31}P{^{1}H} NMR, δ 37.8 (s, 2P, SdppmS).

Crystal structure determinations

The crystals were mounted in inert oil on glass fibres and transferred to the cold gas stream of a Siemens P4 diffractometer equipped with an Oxford (**3**,**8**) or Siemens LT-2 (**4**) low temperature attachment. Data were collected using monochromated Mo-Kα radiation (λ = 0.71073 Å). Scan type θ–2θ (**3**,**8**) or ω (**4**). Cell constants were refined from setting angles of *ca.* 60 reflections in the range 2θ 10–25°. Absorption corrections were applied on the basis of ψ-scans. Structures were solved by direct methods and refined on F^2 using the program SHELXL-93 (**4**) or SHELXL-97.[22] All non-hydrogen atoms were refined anisotropically. Hydrogen atoms were included using a riding model. A systems of restraints to light-atom displacement-factor components and local ring symmetry was used (compounds **4** and **8**). The structure of **4** contains a region of badly resolved electron density probably corresponding to a hexane molecule disordered over an inversion centre. Because this solvent could not be unambiguously identified, it is not included in the formula and derived parameters in the crystallographic table. The structure of complex **8** contains five chloroform molecules, one of which is disordered over an inversion centre. Further crystallographic details are given in Table 5.

CCDC reference numbers 165748–165750.

See http://www.rsc.org/suppdata/dt/b1/b102636b/ for crystallographic data in CIF or other electronic format.

Acknowledgements

We thank the Dirección General de Investigación Científica y Técnica (No. PB97-1010-C02-01), the Caja de Ahorros de la Inmaculada (No. CB4/98) and the Fonds der Chemischen Industrie for financial support.

References

1 *Ferrocenes, Homogeneous Catalysis, Organic Synthesis and Materials Science*, ed. A. Togni and T. Hayashi, VCH, Weinheim, 1995.

2 *Metallocenes*, ed. A. Togni and R. L. Halterman, VCH, Weinheim, 1998.

3 N. J. Long, *Metallocenes*, Blackwell, Oxford, 1998.

4 P. D. Beer, P. A. Gale and G. Z. Chen, *J. Chem. Soc., Dalton Trans.*, 1999, 1897.

5 C. Valério, J. L. Fillaut, J. Ruiz, J. Guittard, J. C. Blais and D. Astruc, *J. Am. Chem. Soc.*, 1997, **119**, 2588.

6 J. D. Carr, S. J. Coles, W. W. Hassan, M. B. Hursthouse, M. A. Malik and J. H. R. Tucker, *J. Chem. Soc., Dalton Trans.*, 1999, 57.

7 B. McCulloch, D. L. Ward, J. D. Woolins and C. H. Brubaker, Jr., *Organometallics*, 1985, **4**, 1425.

8 S. Coco and P. Espinet, *J. Organomet. Chem.*, 1994, **484**, 113.

9 V. C. Gibson, N. J. Long, A. J. P. White, C. K. Williams and D. J. Williams, *Chem. Commun.*, 2000, 2359.

10 V. C. Gibson, N. J. Long, A. J. P. White, C. K. Williams and D. J. Williams, *Organometallics*, 2000, **19**, 4425.

11 M. C. Gimeno and A. Laguna, *Gold Bull.*, 1999, **32**, 90 and references cited therein.

12 M. Munakata, S. G. Yan, M. Maekawa, M. Akiyama and S. Kitagawa, *J. Chem. Soc., Dalton Trans.*, 1997, 4257.

13 E. M. Barranco, O. Crespo, M. C. Gimeno, P. G. Jones, A. Laguna and M. D. Villacampa, *J. Organomet. Chem.*, 1999, **592**, 258.

14 E. M. Barranco, O. Crespo, M. C. Gimeno, A. Laguna, P. G. Jones and B. Ahrens, *Inorg. Chem.*, 2000, **39**, 680.

15 L. Carlucci, G. Ciani, D. M. Proserpio and A. Sironi, *J. Am. Chem. Soc.*, 1995, **117**, 4562.

16 P. Zanello, G. Opromolla, G. Giorgi, G. Sasso and A. Togni, *J. Organomet. Chem.*, 1996, **506**, 61.

17 P. D. Beer, C. Blackburn, J. F. McAleer and H. Sikanyika, *Inorg. Chem.*, 1990, **29**, 378.

18 J. D. Carr, S. J. Coles, M. B. Hursthouse, M. E. Light, E. L. Munro, J. H. R. Tucker and J. Westwood, *Organometallics*, 2000, **19**, 3312.

19 R. Usón, A. Laguna, M. U. de la Orden and M. L. Arrese, *Synth. React. Inorg. Met.-Org. Chem.*, 1984, **14**, 369.

20 R. Usón, A. Laguna, M. Laguna, J. Jiménez and E. Durana, *Inorg. Chim. Acta*, 1990, **168**, 89.

21 R. Usón and A. Laguna, *Inorg. Synth.*, 1982, **21**, 71.

22 G. M. Sheldrick SHELXL-93/SHELXL-97, Program for Crystal Structure Refinement, University of Göttingen, Germany, 1993/1997.